IEEE Access
Multidisciplinary | Rapid Review | Open Access Journal

Received March 2, 2021, accepted April 1, 2021, date of publication April 7, 2021, date of current version April 19, 2021.

Digital Object Identifier 10.1109/ACCESS.2021.3071463

Optimal Planning Method for Power System Line Impedance Based on a Comprehensive Stability Margin

DAHU LI[1,2], SHUAI YANG[1], WENTAO HUANG[1], JUN HE[1], (Member, IEEE), ZHIJUN YUAN[1], AND JINMAN YU[1]

[1]Hubei Key Laboratory for High-Efficiency Utilization of Solar Energy and Operation Control of Energy Storage System, Hubei University of Technology, Wuhan 430068, China
[2]State Grid Hubei Electric Power Company Ltd., Wuhan 430077, China

Corresponding authors: Wentao Huang (280515123@qq.com) and Jun He (apm874@163.com)

This work was supported in part by the High-Level Talent Fund of Hubei University of Technology under Grant BSQD2019013.

ABSTRACT With the increasing scale of power systems and the large-scale application of new energy technologies, the planning and construction of future power grids and the stable operation of systems face severe challenges. Among them, transient stability and short-circuit current are two key factors that determine the safe and stable operation of a power system. However, in traditional power-grid planning, there is little research on the strategy of coordinating the solution between transient stability, short-circuit current problems and planning forecasts. Based on the perspective of power-grid planning, this study proposes a method for the optimal planning of a power system's comprehensive stability margin that uses the external penalty function method. The coupling relationship between the transient stability margin and short-circuit current margin is developed through the system impedance in power-grid planning, and the line impedance optimization planning problem based on the comprehensive stability margin is formulated as a multiobjective optimization model. Finally, the optimal system impedance and the optimal comprehensive stability margin are determined by the external penalty function method. The simulation results of an IEEE 10-generator 39-bus system verify the effectiveness of the proposed method, and the system with the optimal planned impedance determined by this method yields the best comprehensive stability margin. Further simulation verification is conducted in a real power grid in China, and the strategy proposed in this article exhibits good economy and scalability. It provides a theoretical basis for the planning and construction of the future power grid, which is conducive to the safe and stable operation of the future power grid.

INDEX TERMS Comprehensive stability margin, power-grid planning, external penalty function method, optimal system impedance value.

I. INTRODUCTION

With the integration of new large-scale energy sources and the expansion of grid interconnections, the planning and construction of future power systems will face more severe tests [1]. Transient instability and excessive short-circuit current are high-frequency faults in power system operation that are closely related to whether the power-grid planning is reasonable. When performing power-supply reliability analysis during grid scheme optimization in traditional grid planning, the sufficiency of the system's power supply and steady state security are typically considered most important [2], and there is less consideration of system transient stability and short-circuit current issues. In this case, the calculated reliability index will be too optimistic to evaluate the planning scheme. Therefore, taking corresponding measures in the planning stage to conduct a scientific and reasonable assessment of transient stability and short-circuit current can improve power-grid planning, ensuring the safe and stable operation of the power system [3].

Currently, few specific solutions have been proposed in the literature to simultaneously solve transient stability and short-circuit current problems. From a planning perspective, a two-stage optimization method is proposed for optimal

The associate editor coordinating the review of this manuscript and approving it for publication was Fabio Mottola.

distributed-generation (DG) planning that considers the integration of energy storage, and the integration of energy storage makes DG operate at its predesigned rated capacities with a probability of at least 60% [4], [5] uses the impedance matrix to linearly express the short-circuit current of the node, and proposes a transmission network planning model that considers the short-circuit current limit. If the impact of the short-circuit current on system stability is fully considered in the planning stage, a scientific assessment and then planning of the grid will be more futureproof. Regarding excessive short-circuit current in the grid, [6] provides an optimized configuration scheme that considers the installation of current-limiting reactors, busbar split operation and other power system current-limiting measures to reduce the short-circuit current in the grid more economically. That paper shows that by optimizing the division of the power grid, the problem of excessive short-circuit current in the division can be solved, and the reliability and scalability of the division operation can be satisfied. Reference [7] shows that the problem of excessive short-circuit current in a division can be solved by optimizing the division of the power grid, and the reliability and scalability of the division operation can be satisfied. In [8], short-circuit current limits were added as a control quantity to the traditional transmission grid planning model, and a two-level expansion planning model was developed for transmission grids in which the short-circuit current limit was considered. Finally, an overall planning scheme was obtained that satisfied the short-circuit current level requirements. To limit the short-circuit current from the planning level, [9] proposes the model-free emergency SIME (E-SIME) method for real-time transient stability prediction by replacing generator variables in a SIME time-domain simulation with a PMU real-time measurement. However, the E-SIME method has a low reliability, is not suitable for multiple swing instability scenarios, and easily misjudges a transient instability as an unstable situation. Reference [10] added the short-circuit current level as a control variable to the optimal power flow model to improve allocation of newly added generator capacity and to describe the economic and reliable operation of the power grid by ensuring a short-circuit current margin. In general, the optimization of the network structure and the application of current limiting measures are considered most important in studies of short-circuit current level control after a power grid has been constructed. However, there are few in-depth studies and applications of how to optimize the impact of short-circuit current in the formation of power-grid planning schemes. Traditional transmission network planning conducts short-circuit current verification after the grid structure is determined but ignores the important guiding role of short-circuit current in grid optimization planning. Traditional transmission network planning also fails to consider the application of current limiting measures at the grid planning level. During grid planning, reasonable planning of line impedance and current limiting measures ensure the safety and reliability of the grid, and retain a certain short-circuit current margin, which improves the long-term sustainable and reliable development of the grid. Regarding power system transient stability, many studies have assessed whether transient stability is possible. However, few studies have investigated the quantitative description of the transient stability margin. Predicting the stability margin of a system is more beneficial to the security defense control of the system [11]. In [12], the mapping relationship between a generator's kinetic energy, power angle, angular velocity, angular acceleration and other characteristic quantities, and limit excision time is constructed using a compound neural network to provide a system stability margin; however, the real-time requirement of the information acquisition system is high. A novel PRTSA approach based on an ensemble of OS extreme learning machines (EOS-ELMs) with binary Jaya (Bin Jaya)-based feature selection is proposed for use with phasor measurement unit (PMU) data [13], which can be used to predict the transient and stable state of a power system. Reference [14] constructed a motion equation for an interconnected power system with renewable energy generation (RPG), and then the transient energy function was derived to analyze the effect of virtual inertia on the transient energy conversion. In [15], a large amount of data was trained through a combination of stacking noise reduction autoencoders and support vector machine integrated models, and the mapping relationship was constructed between the pre-fault power flow and transient stability margins, such as line power, generator output, bus voltage, and load. This relationship belongs to the transient stability assessment under the concept of a safe domain, and its model is complex. After training with a large amount of data, this model can effectively characterize complex functions. In [16], via a multistep Lasso method, the mapping relationship between the limited resection time and the steady-state operating voltage and phase angle can be developed to effectively remove irrelevant variables. Training with a small amount of data can achieve better prediction results; however, because the simple model changes when the system operation mode changes, the prediction error increases when the limit cutting time changes. From the perspective of voltage stability analysis, a novel system method for dynamic reactive power planning is proposed to provide decision makers with more Pareto optimal solutions to improve short-term voltage stability and transient stability [17]. Thus, a robust dynamic VAR programming method is proposed to improve short-term voltage stability level under the condition of unexpected events when uncertainty occurs [18], [19] builds an integrated learning model based on a neural network with random weights to achieve short-term voltage stability evaluation. In [20], aiming at the power system with a high proportion of renewable energy access, a two-stage stochastic optimization model is established that takes into account both the network structure optimization and the energy storage configuration. While ensuring the transient stability of the power grid, it also improves the economy and safety level of system operation.

In [21], in the power grid expansion plan, the dynamic capacity increase of the line and the optimization measures of the transmission grid structure are considered at the same time, with the goal of minimizing the sum of the system construction cost and operating cost. Reference [22] from a planning perspective, the transmission capacity constraints of the line and the carbon emission reduction constraints of the system are included in the planning model, and the objective function is to minimize equipment investment and system operation and maintenance costs. Reference [23] established a method to optimize the structure of the transmission grid to ensure the utilization of wind power. The results show that the optimization of the transmission grid structure plays an important role in improving the transient stability of the system. These studies of power-grid planning have some applicable value. However, the power-grid planning scheme proposed in this paper focuses on optimizing the planning of power grid line impedance, which has a strong impact on a system's power angle stability. As the scale of a power system increases, the problems of power angle stability and short-circuit current overload will become more prominent; thus, this paper focuses on power angle stability with regard to transient stability.

In this paper, from the perspective of power-grid planning, a coordinated optimization objective function is developed to characterizes the power grid stability level for the first time and provide constraints based on the transient stability margin and short-circuit current margin. A control strategy based on the external point penalty function method to solve the optimal system stability margin is also proposed to ensure the stable operation of the system. This strategy simultaneously solves the problems of transient stability and short-circuit current in the power system by optimizing the best stability margin of the system. The example simulation verification with an IEEE 10-generator 39-bus system demonstrates that the strategy proposed in this paper can effectively improve the system's comprehensive stability margin. Lastly, a case study was performed in an real power grid in China, and the calculated costs of various schemes were compared to show that the proposed strategy exhibits good scalability and economy. This study provides a theoretical basis for future grid planning, construction and operation, thereby improving the safety and stability of the power system.

II. POWER GRID LINE PLANNING BASED ON STABILITY MARGIN

A. LINE CORRIDOR

During power-grid planning, the path planning of the AC line corridor between the two substations has an impact on line length and impedance when the distribution of substations is determined. During planning, economic principles must be considered, in addition to considering the economics of the planning scheme, and the AC line length must be optimized within a certain range so that the best AC line impedance for the safe and stable operation of the power grid can be optimized. Considering the conditions of any two substations, the AC lines between two sites have different corridor planning forms. As shown in Figure 1.

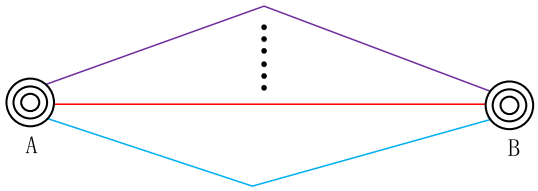

FIGURE 1. Schematic diagram of various forms of route corridors.

Assuming that the impedance from substations A to B is X_{AB} under the conditions of meeting environmental issues, corridor land, and construction costs, the size of X_{AB} can be adjusted within a certain range based on specific planning:

$$X_{AB\,\min} \leq X_{AB} \leq X_{AB\,\max} \tag{1}$$

When planning an entire power grid, power grid operation characteristics can be optimized, including each line length path within a certain range, to obtain the optimal line impedances. Consider a power grid that has N nodes and L transmission lines, as shown in Figure 2:

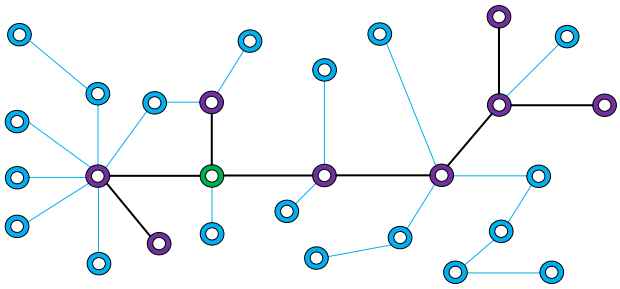

FIGURE 2. Simple power grid schematic diagram.

For this grid, the impedance of each line can be expressed as a matrix:

$$X = [X_1, X_2, X_3 \cdots\cdots X_l] \tag{2}$$

Within the allowable adjustment range of the line corridor, the impedance of any transmission line in the grid has:

$$X_{ij\,\min} \leq X_{ij} \leq X_{ij\,\max} \tag{3}$$

During power-grid planning, it is necessary to fully consider the security and stability of the power grid. Transient stability characteristics and short-circuit current are the two key factors of power system security and stability analysis. These two factors are closely related to the system impedance; the power grid planning scheme in this article is based on the determination of the site selection

of substation sites, assuming that the two substations are connected by AC lines, and the length of the AC line corridor changes within a certain range. Reasonably plan the length of the AC line within the required range to optimize the line impedance value, so as to achieve the purpose of improving the stable operation of the power grid and ensuring the economy. Thus, reasonable optimization of the line corridor is important to the safe and stable operation of the power grid.

B. ANALYSIS OF TRANSIENT STABILITY CHARACTERISTICS

This article focuses on the problem of power-grid planning, particularly the optimization of line impedance, which has a strong impact on the electromechanical transient stability of the power grid. Therefore, this paper ignores the electromagnetic transient process of the power grid.

In the electromechanical transient process simulation, a single-machine infinite bus system is used to simulate the power angle stability process of the power grid to make the mathematical modeling of the objective function more convenient and effective; this is a reasonable simplification that still meets the requirements of power-grid planning. Lyapunov's direct method can be used in the analysis of the transient stability characteristics of the power grid. The specific system transient stability function in [24], [25] can be described as:

$$V = V_k + V_p = \frac{1}{2}M\omega^2 + \int_{\delta_0}^{\delta}(P_e - P_m)d\delta \tag{4}$$

where P_m in the system is the mechanical power and remains constant; V_k is the kinetic energy of the system; V_p is the potential energy of the system; P_e is the electromagnetic power; M is the inertial time constant, ω is the deviation between the rotor angular velocity and the synchronous speed; and δ_0 and δ are the power angles that correspond to the front and rear stable operating points, respectively.

Setting δ_0 as the starting point, the $\omega-\delta$ phase relationship is shown in Figure 3.

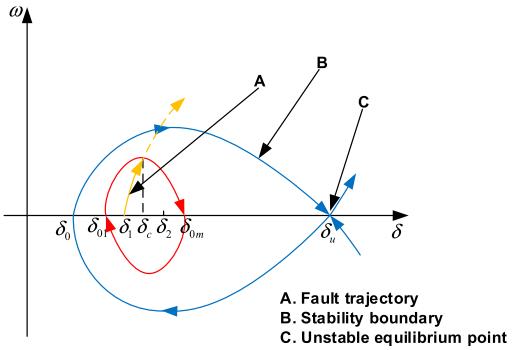

FIGURE 3. $\omega-\delta$ phase relationship diagram.

In Figure 3, δ_2 is the steady-state equilibrium point, where ω is 0, and the trajectory during stable operation is around this point. It is assumed that the system encounters a fault at δ_1, and that the fault clears at δ_c. Without considering damping, the system moves repeatedly along δ_{01} to δ_{0m}. The outer ring indicates the situation when the system is in a critical condition, where δ_u is the critical point (unstable equilibrium point), and when δ crosses δ_u, the system becomes unstable.

At time t_c, the system disturbance ends, the fault clearing angle is δ_c, and the system transient energy is V_c:

$$V_c = \frac{1}{2}M\omega_c^2 + \int_{\delta_s}^{\delta_c}(P'_e - P_m)d\delta \tag{5}$$

where ω_c is the deviation between the rotor angular speed and the synchronous speed at this moment, and P'_e is the electromagnetic power after the fault is removed.

The potential energy when the system is at the unbalanced location is considered to be the critical energy V_{cr}:

$$V_{cr} = \int_{\delta_s}^{\delta_u}(P'_e - P_m)d\delta \tag{6}$$

where δ_u is the power angle when the system is in an unbalanced and stable operation point; and δ_s is the power angle when the system is in a stable operation.

In practical applications, the difference between the critical energy and the transient energy at the end of the disturbance is used to describe the transient stability margin of the system, which can be expressed as follows:

$$S(X) = \frac{V_{cr} - V_c}{V_{k/c}} = \frac{\int_{\delta_s}^{\delta_u-\delta_c}\left(\frac{E'U}{X}\sin\delta - P_m\right)d\delta}{M\omega_c^2} - 1 \tag{7}$$

where $V_{k/c}$ is the kinetic energy at the end of the system disturbance at time t_c. Taking the derivative of $S(X)$, we can find that $S'(X) < 0$. Then, the system equivalent impedance X has a negative correlation with the transient stability margin. Increasing the line impedance reduces the transient stability characteristics of the power system. Conversely, reducing the line impedance can improve the transient stability characteristics of the power system.

C. SHORT CIRCUIT CURRENT ANALYSIS

In the calculation of the short-circuit current of the power system, the initial value I_k'' of the periodic component of the short-circuit current is calculated first and is also referred to as the initial subtransient current. The calculation principle is shown in Figure 4.

This article uses the engineering algorithm to describe a short-circuit current. Ignoring the transition impedance during the short-circuit process, the initial value vector matrix of the periodic component of the short-circuit current of the node is expressed as $\mathbf{I}$:

$$\mathbf{I} = \frac{C\mathbf{U}}{\sqrt{3}\mathbf{X}} \tag{8}$$

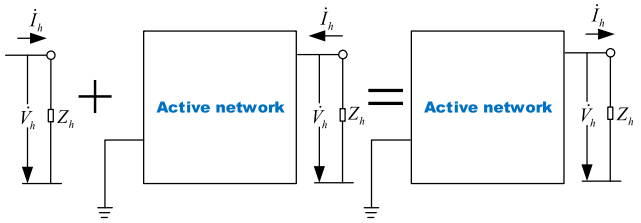

FIGURE 4. Short-circuit current calculation principle diagram.

In Formula (8), where C is the voltage coefficient, the open circuit voltage matrix at the fault point is $\mathbf{U}$:

$$\mathbf{U} = \begin{bmatrix} U_{11} & \cdots & U_{1l} \\ \vdots & \ddots & \vdots \\ U_{l1} & \cdots & U_{ll} \end{bmatrix} \tag{9}$$

The equivalent impedance matrix of the system is $\mathbf{X}$ with unit Ω:

$$\mathbf{X} = \begin{bmatrix} X_{11} & \cdots & X_{1k} \\ \vdots & \ddots & \vdots \\ X_{k1} & \cdots & X_{kk} \end{bmatrix} \tag{10}$$

The interruption current vector matrix of all nodes under the system voltage level is $\mathbf{I}_{\max}$:

$$\mathbf{I}_{\max} = \begin{bmatrix} \mathrm{I}_{\max 1} & & \\ & \ddots & \\ & & \mathrm{I}_{\max w} \end{bmatrix} \tag{11}$$

The real current of the system is $\mathbf{I}_{\mathrm{k}}$:

$$\mathbf{I}_{\mathrm{k}} = \begin{bmatrix} \mathrm{I}_{\mathrm{k}1} & & \\ & \ddots & \\ & & \mathrm{I}_{\mathrm{k}w} \end{bmatrix} \tag{12}$$

The current stability margin index of the system is specified as W:

$$W = \frac{\mathbf{I}_{\max} - \mathbf{I}_k}{\mathbf{I}_{\max}} \times 100\% \tag{13}$$

D. SYSTEM COMPREHENSIVE STABILITY MARGIN

Combined with the short-circuit current engineering algorithm, the short-circuit current margin index is expressed as $W(X)$:

$$W(\mathbf{X}) = \frac{\sqrt{3}\mathbf{I}_{\max}\mathbf{X} - C\mathbf{U}}{\sqrt{3}\mathbf{X}^2} \times 100\% \tag{14}$$

Based on the current margin index, reasonable planning of the system equivalent impedance in the initial stage of power-grid construction can effectively adjust the short-circuit current margin index of the power system. Combining Formulae (7) and (14), the trend of the transient stability margin and short-circuit current margin affected by the system impedance is shown in Figure 5.

Figure 5 shows that the larger the system impedance X is, the short-circuit current value also decreases; however, its

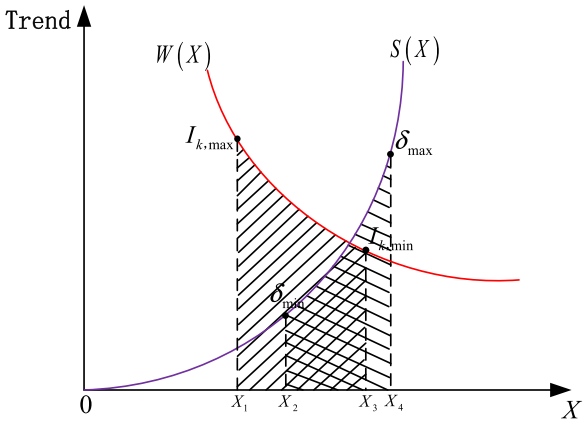

FIGURE 5. Trend of the transient stability margin and short-circuit current margin affected by system impedance.

transient stability level also decreases or loses stability. The smaller the system impedance value is, the transient stability level will rise; however, the short-circuit current value will also increase or exceed its upper current limit. Then, the size of the system impedance X is optimized to ensure that the short-circuit current and transient stability characteristics reach a reasonable level concurrently.

The transient stability level in the system optimization process is represented by the stability margin S, and the short-circuit current margin is represented by W. During power-grid planning and optimization, a comprehensive stability margin is M defined in this paper, the comprehensive stability margin is the concept of power grid stability planning proposed in this paper, which includes short-circuit current margin and transient stability margin. The short-circuit current level and transient stability level of the power grid are used to characterize the safety and stability of the power grid. The comprehensive stability margin M is composed of a transient stability margin S and a short-circuit current margin W. The weight coefficients of the two are λ_1, λ_2, respectively. Then, the comprehensive stability margin of the system is M:

$$M = \lambda_1 S + \lambda_2 W \tag{15}$$

where λ_1 and λ_2 are weight coefficients, and $\lambda_1 + \lambda_2 = 1$, In the general typical power grid, $\lambda_1 = \lambda_2 = 0.5$ is used. The specific values of λ_1 and λ_2 are related to the voltage level, scale, grid structure, and operating characteristics of the power grid. For power grids where transient instability is more destructive to stability, $\lambda_1 \gg \lambda_2$, such as $\lambda_1 = 0.8, \lambda_2 = 0.2$;For power grids where short-circuit current exceeding the standard is more destructive to the stability of the power grid, $\lambda_2 \gg \lambda_1$, such as $\lambda_2 = 0.8, \lambda_1 = 0.2$.

III. SOLVING THE OPTIMAL COMPREHENSIVE STABILITY MARGIN BASED ON THE METHOD OF EXTERIOR POINT PENALTY FUNCTION

This study has theoretically deduced that the key influencing variable of the comprehensive stability margin is the

system impedance, and it is feasible to optimize the system impedance through the algorithm to obtain the maximum stability margin of the system. When seeking the optimal system impedance, the general elimination method cannot solve the constraint nonlinear problem in the process. To meet these constraints and minimize the objective function value, which determines the optimal system impedance, it is necessary to use the minimization auxiliary function to convert the constrained nonlinear problem into an unconstrained problem. The method proposed in this paper may be sensitive to its primary control parameters. To mitigate this issue, this paper uses the external point penalty function method to establish an objective function that links the transient stability and short-circuit current; considers system parameters and transient energy expressions as constraints; and establishes a penalty function to mitigate the model's sensitivity to changes in parameters to improve the optimization method. Thus, this paper uses the exterior point penalty function method to determine the optimal system impedance [26], [27].

A. ALGORITHM PRINCIPLE

The principle of the external point penalty function is to construct a penalty function based on the characteristics of the constraint, which is then added to the objective function to convert the constraint problem into a series of unconstrained problems. This ''penalty strategy'' will punish target points that attempt to violate the constraints during solving unconstrained problems, as shown in Figure 6.

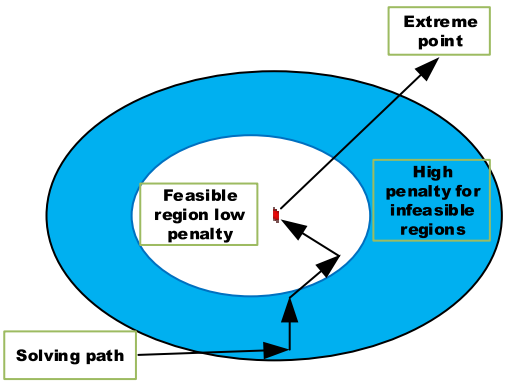

FIGURE 6. Schematic diagram of the exterior point penalty function method.

The external point penalty function constraint problem is:

$$\begin{cases} \min f(x), & x \in R^n \\ s.t.\ g_i(x) \geq 0, & i = 1, 2, \ldots, u \\ h_j(x) = 0, & j = 1, 2, \ldots, w \end{cases} \tag{16}$$

where $f(x)$, $g_i(x)$, $h_j(x)$ is a continuous function on R^n with the equality constraints:

$$\begin{cases} \min f(x) \\ s.t.\ h_j = 0, \quad j = 1, 2, \ldots, l \end{cases} \tag{17}$$

We define the auxiliary function as:

$$F_1(x, \sigma) = f(x) + \sigma \sum_{j=1}^{l} h_j^2(x) \tag{18}$$

The parameter σ is a large positive number, and Formula (18) can be transformed into an unconstrained problem:

$$\min F_1(x, \sigma) \tag{19}$$

The form of the auxiliary function is different from the equality constraint; however, the basic idea of constructing the auxiliary function is the same. When in the feasible region, the auxiliary function is equal to the developed objective function value. At an infeasible point, its value is equal to the objective function value plus a great positive number:

$$F_2(x, \sigma) = f(x) + \sigma \sum_{i=1}^{m} [\max\{0, -g_i(x)\}]^2 \tag{20}$$

where σ is a large positive number. Additionally, when x is a feasible point:

$$\max\{0, -g_i(x)\} = 0 \tag{21}$$

When x is an infeasible point:

$$\max\{0, -g_i(x)\} = -g_i(x) \tag{22}$$

Converting Formula (20) into a constraint problem yields:

$$\min F_2(x, \sigma) \tag{23}$$

Extending these ideas to include general conditions, functions can be defined as $F(x, \sigma)$:

$$F(x, \sigma) = f(x) + \sigma P(x) \tag{24}$$

where $P(x)$ has the following form:

$$P(x) = \sum_{i=1}^{m} \phi(g_i(x)) + \sum_{j=1}^{l} \psi(h_j(x)) \tag{25}$$

B. ESTABLISH THE OPTIMIZATION MODEL

1) EXTERNAL PENALTY FUNCTION N

During power-grid planning, the system impedance can affect the comprehensive stability margin of the system. It is thus necessary to fully consider the impact of the system impedance on the system transient stability and the impact on the short-circuit current level under the condition of meeting the breaking capacity of the circuit breaker. Therefore, the line impedance optimization planning problem based on the comprehensive stability margin is formulated as a multiobjective optimization model that seeks transient stability without exceeding the short-circuit current and the best comprehensive stability margin of the system. To solve the optimization model, an objective function sequence with a penalty effect is constructed, and large objective function values are given to those iterative points that attempt to violate

constraints in the solution process. The minimum point of this series of unconstrained problems is forced to approach the admissible set infinitely until it converges to the minimum point of the constrained problem, thereby ensuring the global optimal solution. Because the optimal comprehensive stability margin in the real power grid is below 100%, and the optimization algorithm requires a minimum value, the objective function is defined as follows:

$$N(X) = 1 - M(X) \tag{26}$$

Optimizing $N(X)$ as the objective function, the objective function can be written as follows:

$$F = \min[N(X)] \tag{27}$$

2) EQUALITY CONSTRAINTS

Requisite equality constraints are described as:

$$\begin{cases} h_{j1} = I_k - \dfrac{CU}{\sqrt{3}X} \\ h_{j2} = V - \dfrac{1}{2}M\omega^2 + \int_{\delta_0}^{\delta}(P_e - P_m)d\delta \\ h_{j3} = V_c - \dfrac{1}{2}M\omega_c^2 + \int_{\delta_s}^{\delta_c}\left(P_e^{(3)} - P_m\right)d\delta \\ h_{j4} = V_{cr} - \int_{\delta_s}^{\delta_u}\left(P_e^{(3)} - P_m\right)d\delta \end{cases} \tag{28}$$

3) INEQUALITY CONSTRAINTS

Requisite inequality constraints are described as:

$$\begin{cases} U_{l,\min} \le U_l \le U_{l,\max}, & l = 1, 2, 3 \cdots n \\ P_{m,\min} \le P_m \le P_{m,\max}, & m = 1, 2, 3 \cdots p \\ \delta_{v,\min} \le \delta_v \le \delta_{v,\max}, & v = 1, 2, 3 \cdots q \\ I_{w,\min} \le I_w \le I_{w,\max}, & w = 1, 2, 3 \cdots r \\ X_{k,\min} \le X_k \le X_{k,\max}, & k = 1, 2, 3 \cdots t \end{cases} \tag{29}$$

where $U_{l,\max}$, $P_{m,\max}$, $\delta_{v,\max}$, $I_{w,\max}$, and $X_{k,\max}$ are the maximum values of the system voltage, generator output, power angle, short-circuit current, and system impedance, respectively; and $U_{l,\max}$, $P_{m,\min}$, $\delta_{v,\min}$, $I_{w,\min}$, and $X_{k,\min}$ are the system voltage, generator output, minimum value of the power angle, short-circuit current and system impedance, respectively.

4) OPTIMIZATION

Based on the calculation steps of the external penalty function, the optimization of $N(X)$ is described in the following steps:

Step 1 (Setting the Objective Function and Constraint conditions): Considering $N(X)$ as the objective function of optimization and the system transient energy function, system potential energy, generator power angle and system impedance value as constraints, the following mathematical model is developed:

$$\begin{cases} F = \min\left[N\left(X^{(k)}\right)\right] \\ s.t.\ h_j(x) = 0, j = 1, 2, \ldots, w \\ \quad g_i(x) \ge 0,\ i = 1, 2, \ldots, u \end{cases} \tag{30}$$

where $h_j(x)$ and $g_i(x)$ are represented by Formulae (28) and (29), respectively.

Based on Formulae (7), (14), and (15), $N(X)$ through the optimal comprehensive margin $M(X)$ is expressed as:

$$N(X) = 1 - \lambda_1 \frac{\int_{\delta_s}^{\delta_u - \delta_c}\left(\frac{E'U}{X}\sin\delta - P_m\right)d\delta}{M\omega_c^2} + \lambda_1 - \lambda_2 \frac{\sqrt{3}I_{\max}X - CU}{\sqrt{3}X^2} \times 100\% \tag{31}$$

Step 2 (Transforming the Objective Function Into an Unconstrained Extreme Value Problem): Based on the objective function combined with constraint conditions, the objective function can be transformed into an unconstrained extreme value solution problem, and an unconstrained extreme value solution function is developed:

$$\min f(X) + \sigma h(X), \quad j \in 1, 2, \ldots, w \tag{32}$$

where X is a set of numbers and an array of system impedance values under each line corridor mode:

$$X = \left[X^{(k-1)}, \ldots, X^n\right], \quad k = 1, \ldots, n \tag{33}$$

Step 3 (Setting Initial Values to Begin Iteration): Let $k = 1$. Then, given that the initial point $X^{(0)}$ and the initial penalty factor σ_1, of which $X^{(0)}$ may not be a feasible point, exist, $\sigma_1 = 1$, the magnification factor is $c > 1$, and the allowable error is $\varepsilon > 0$. Among these values, $\varepsilon = 10^{-4}$ and $c = 10$ are substituted into Formula (32) to obtain the minimum value. The partial derivative of $X^{(k)}$ is considered to be the minimum value when the partial derivative is 0:

$$\frac{d\left(f(X^{(k)}) + \sigma h(X^{(k)})\right)}{d(X^{(k)})} = 0 \tag{34}$$

Step 4 (Obtaining the Corresponding $X^{(k)}$): If $\sigma_k h(X^{(k)}) < \varepsilon$, then $X^{(k)}$ is the approximate optimal solution, the calculation is stopped, $N(X^{(k)})$ is calculated, and $M(X^{(k)})$ is determined to be the optimal system comprehensive stability margin. Otherwise, $\sigma_{k+1} = c\sigma_k$, $k = k + 1$, and the process returns to Step 3.

The process of solving the optimal system comprehensive stability margin is shown in Figure 7.

IV. ANALYSIS OF EXAMPLE

A. CASE 1–IEEE 39-BUS SYSTEM

This paper uses the IEEE 10-generator 39-bus system calculation example to verify the proposed model. Figure 8 shows the numbers of generators and buses in the IEEE 10-generator 39-bus system. This example is used to calculate the comprehensive stability margin of the system. Based on the characteristics of the power grid structure in the IEEE 10-generator 39-bus system, λ_1 and λ_2 are both set to 50%, and this example is used to test the effect of the impedance optimization scheme proposed in this paper.

In this paper, the data of the IEEE 10-generator 39-bus system calculation example use per-unit values. First, using

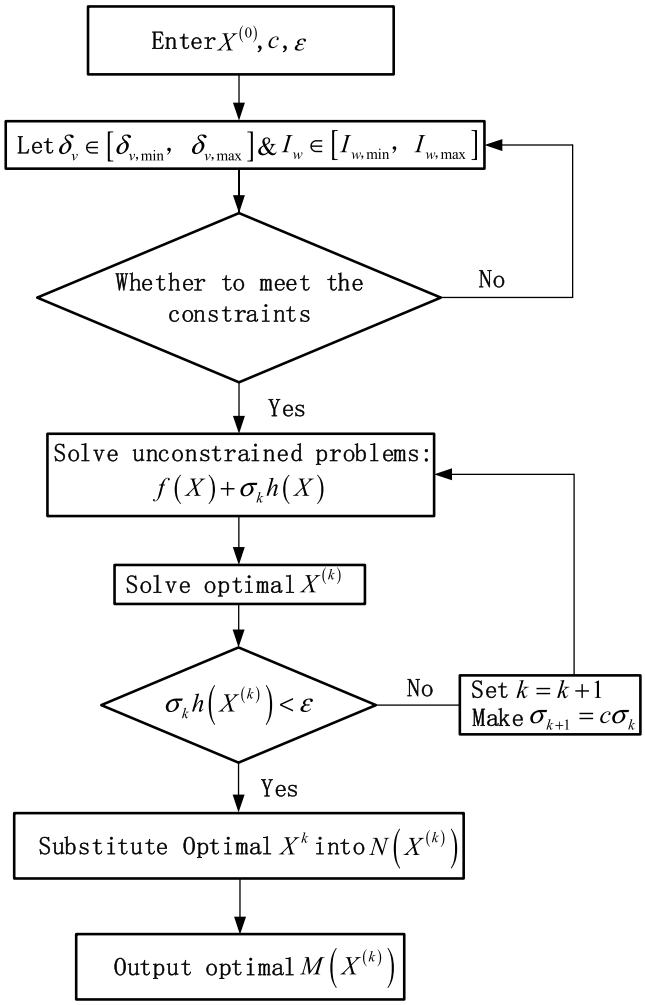

FIGURE 7. Optimal system comprehensive stability margin solution process.

TABLE 1. Impedance schemes for certain lines of IEEE 10-generator 39-bus.

Head end substation	Terminal substation	Optimization scheme	scheme 1	scheme 2	scheme 3
13	12	0.032	0.028	0.034	0.037
13	10	0.032	0.028	0.039	0.036
15	16	0.085	0.069	0.079	0.090
16	24	0.076	0.072	0.089	0.082
6	11	0.053	0.063	0.056	0.069

the MATLAB 2016b simulation platform, the system parameters are substituted into the optimization model defined above to obtain a set of optimal system impedances that meet line-planning requirements and are set as the optimization scheme. Three sets of impedances are randomly selected within the allowable impedance range of the planned line to form three comparison schemes. The optimized scheme in this paper is compared to the simulation results of three other schemes. The impedances of certain lines in the IEEE 10-generator 39-bus system example under the optimized scheme and the three comparison schemes are shown in Table 1.

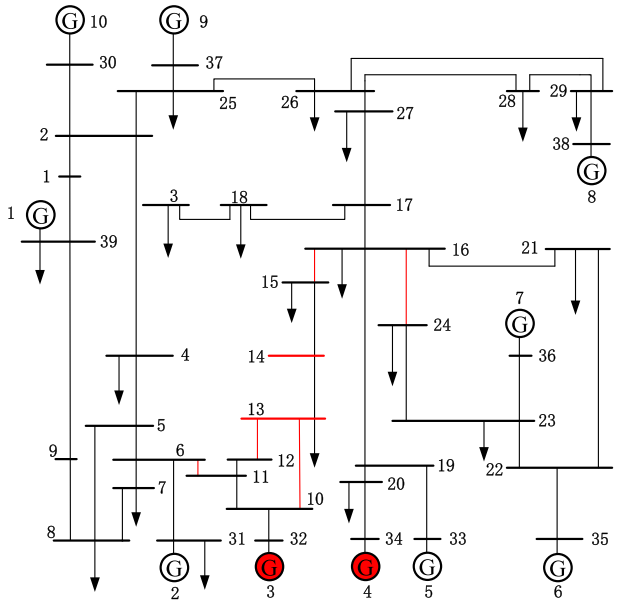

FIGURE 8. IEEE 10-generator 39-bus system.

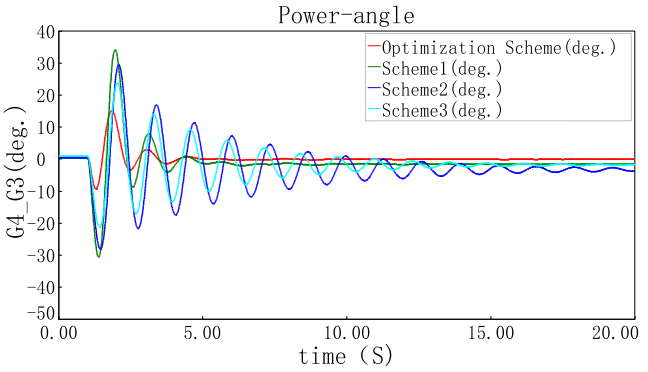

FIGURE 9. Unit power angle curve.

Based on the IEEE 10-generator 39-bus system grid structure, the parameters of the system are substituted into the Power System Analysis Software Package (PSASP), which is a set of power system analysis programs developed by the China Electric Power Research Institute. PSASP is a large-scale software package that provides resource sharing and is easy to use, highly integrated and open-source. This software package performs three-phase short circuit fault and disconnection fault simulation verification on lines 14-15. Taking the power angle of the generator set numbered G3 and the relative power angle of the generator set numbered G4 as observation objects, the frequency of bus No. 13 is used as the system frequency observation object, and the voltage of bus No. 14 is considered to be the system voltage observation object. Lines are marked in red in Figure 8, and the G3 generator power angle, the frequency of the 13 buses, and the voltage of the 14 buses under the 4 impedance value schemes are obtained, as shown in Figures 9-11, respectively.

The four power angle curves in Figure 9 represent the changes in the power angle in the system under the four

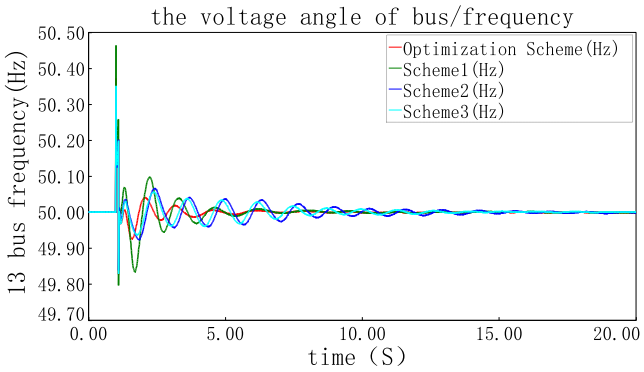

FIGURE 10. Frequency fluctuations of bus 13.

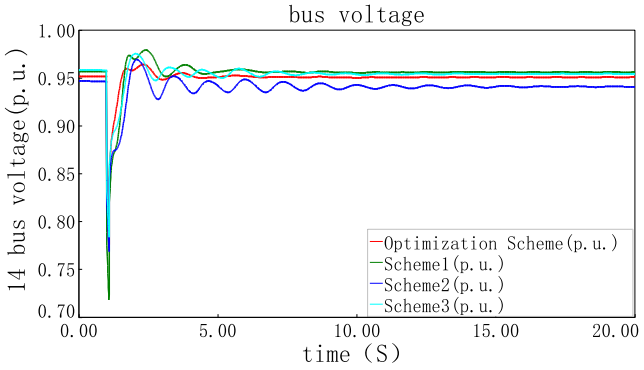

FIGURE 11. Voltage of bus 14.

impedance conditions after encountering the abovementioned faults. Under scheme 1 conditions, although the power angle quickly stabilizes, the amplitude of the first change in the unit power angle curve is relatively large. Under the conditions of schemes 2 and 3, the amplitude of the power angle curve is large, and the power angle fluctuates sharply, requires a long time to stabilize, and could easily make the system unstable. Under optimization scheme conditions, the power angle amplitude is small, and the unit quickly enters stable operation. The power angle curve under the optimized scheme has a smaller amplitude than the three power angle curves under the conditions of schemes 1-3 and tends to become stable more quickly (i.e., the transient stability is better).

The simulation results shown in Figures 10 and 11 are similar to the change in the generator power angle. The system frequency and bus voltage under the optimization scheme exhibit smaller fluctuations and are more stable than those of the other three impedance schemes. The transient stability of the system under the optimized scheme impedance is significantly better than that of the other three schemes.

Additionally, short-circuit faults are set for the 13 buses, and short-circuit calculations are performed on the system. The system's short-circuit current was determined under each impedance scheme, as shown in Table 2.

Substituting the parameters of the system into $S(X)$ and $W(X)$ can yield the transient stability margin and short-circuit current margin under the 4 schemes.

TABLE 2. Short-circuit current under each impedance scheme with the IEEE 10-generator 39-bus system (unit: kA).

	Optimization scheme	scheme 1	scheme 2	scheme 3
Short circuit current	31.99	39.50	36.67	31.56

TABLE 3. Transient stability margin, short-circuit current margin, and comprehensive stability margin under each impedance scheme with the IEEE 10-generator 39-bus system.

Margin	Optimization scheme	scheme 1	scheme 2	scheme 3
Transient stability margin	68.52%	46.64%	12.28%	10.26%
Short circuit current margin	56.32%	26.58%	36.36%	58.42%
Comprehensive stability margin	62.42%	36.61%	24.32%	34.34%

Concurrently, the comprehensive stability margin of the system can be obtained by substituting the system parameters under the four schemes into the optimization model defined above, as shown in Table 3.

Based on the calculated results shown in Table 3 and by comparing the optimization scheme with the other three comparison schemes, the transient stability margin and the short-circuit current margin may not both be optimal concurrently under the conditions of the optimization scheme. However, the overall stability margin of the system is maximized, which is conducive to the safe and stable operation of the system. Using the optimization model developed in this paper, the optimal system impedance and comprehensive stability margin are calculated using the external penalty function method and then substituted into the IEEE 10-generator 39-bus system example for power grid simulation, verifying the effectiveness of the strategy proposed in this paper.

B. CASE 2–REAL POWER SYSTEM OF A PROVINCE IN CHINA

To test the scalability of this method and its applicability in real systems, and compare the calculated cost of this method to further ensure economy, we investigate a real power grid in a province of China as an example and calculate using data from actual power grid. Based on the characteristics of the real power grid structure, λ_1 and λ_2 are both set equal to 50%. The 220-kV grid frame of this power grid is shown in Figure 12. Substations are numbered separately, and the red line is the key simulation analysis line.

In this paper, the data of the real power grid in a province of China uses per-unit values. First, system parameters are substituted into the optimization model defined above to obtain a set of optimal system impedances that meet the line-planning requirements and are set as the optimization scheme. Three sets of impedances are randomly selected within the allowable impedance range of the planned line to

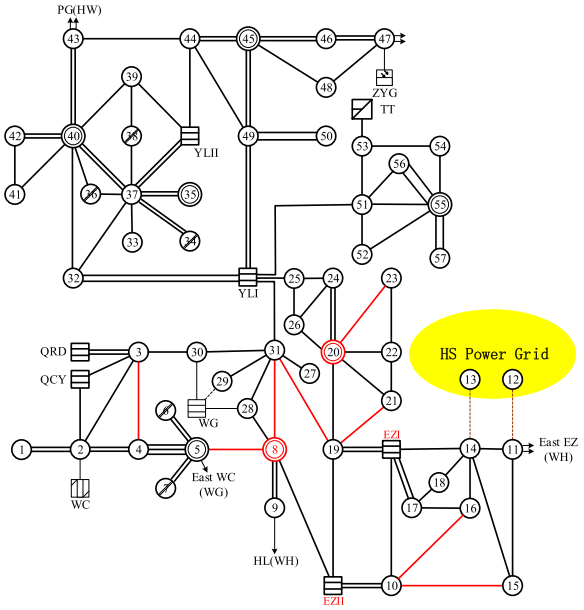

FIGURE 12. Part of the real grid system.

TABLE 4. Impedance schemes for certain lines of a real power grid in a province of china.

Head end substation	Terminal substation	Optimization scheme	scheme 1	scheme 2	scheme 3
3	4	3.18	2.88	3.36	3.09
5	8	4.25	4.92	4.31	4.8
8	31	3.32	3.81	3.76	3.28
31	19	7.10	6.87	7.52	6.96
20	23	0.42	0.40	0.38	0.38
19	21	3.76	3.35	4.21	3.80
10	16	3.12	3.10	2.93	3.42
10	15	20.56	21.72	20.88	19.60

form three comparison schemes. The optimized scheme in this paper is compared to the simulation results of a comparison scheme. The impedances of certain lines in the 220 kV primary grid of the real power grid are shown under the optimized scheme and three comparison schemes in Table 4.

Based on the real power grid, the parameters of the system are substituted into PSASP, and three-phase short circuit fault and disconnection fault simulation verification is performed on lines 19-20. Taking the power angle of the generator set numbered EZI and the relative power angle of the generator set numbered EZII as observation objects, the frequency of bus 20 is used as the system frequency observation object, and the voltage of bus 8 is considered to be the system voltage observation object. The lines are marked in red in Figure 12. The EZI generator power angle, the frequency of bus 20, and the voltage of bus 8 under the 4 impedance schemes are obtained, as shown in Figures 13-15, respectively.

Figure 13 is the power angle curve of the generator under the 4 schemes within the allowable adjustment range of

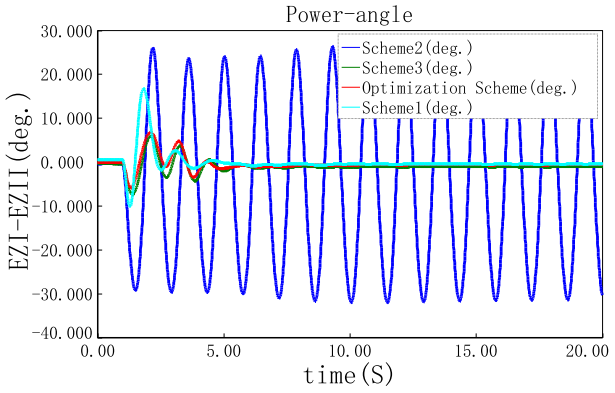

FIGURE 13. Unit power angle curve.

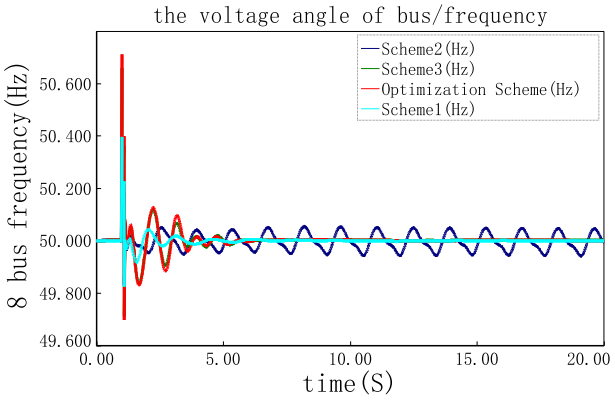

FIGURE 14. Frequency fluctuations of bus 8.

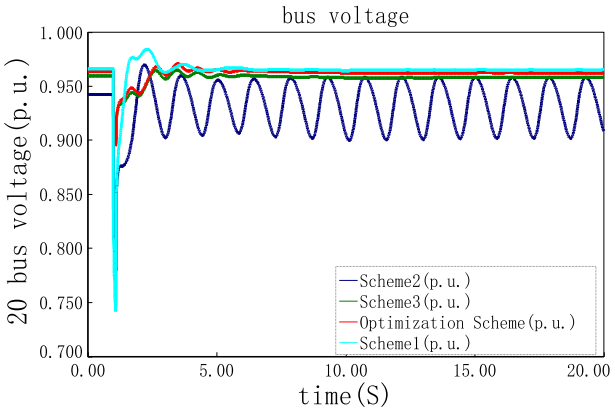

FIGURE 15. 20 bus voltage.

the planned line impedance. Among them, the power angle curve under the Scheme2 condition has an equal-amplitude oscillation. Obviously, the stable operation of the system is easily damaged under this scheme. Although the system still remains transiently stable under the conditions of Scheme1 and Scheme3, but compared with the Optimization Scheme, under the optimization scheme, the power angle amplitude is smaller, and the unit quickly enters stable operation, that is, the transient stability is better.

From the simulation results shown in Figures 14 and 15, the system frequency and bus voltage fluctuations are found to be smaller and more stable under the optimization scheme. The transient stability of the system under the optimization scheme is significantly better than that of the other three schemes.

Substituting the parameters of the system into $S(X)$ and $W(X)$, the average construction cost per unit length of the line is M under the influencing factors of the specific line type and operating environment in this area. The transient stability margin, short-circuit current margin, comprehensive stability margin and line planning cost of the system under the 4 impedance value schemes are shown in Tables 5 and 6.

TABLE 5. Short-circuit current under 4 impedance schemes (unit: kA).

	Optimization scheme	scheme 1	scheme 2	scheme 3
Short circuit current	28.36	35.43	29.69	40.21

TABLE 6. Transient stability margin, short-circuit current margin, comprehensive stability margin and line planning cost under each impedance scheme of a given power grid.

Margin	Optimization scheme	scheme 1	scheme 2	scheme 3
Transient stability margin	66.56%	39.35%	4.65%	68.33%
Short circuit current margin	43.28%	29.14%	40.62%	10.58%
Comprehensive stability margin	54.92%	34.25%	22.64%	39.46%
Line planning cost	932 M	1183 M	1095 M	956 M

Tables 4 and 5 show that the short-circuit current of the optimized scheme is below that of schemes 1 and 3, and the difference in the short-circuit current between the optimized scheme and scheme 2 is small. The transient stability margin of the optimized scheme is much higher than the transient stability margins of schemes 1 and 2; however, the transient stability margin of scheme 3 is marginally better than that of the optimized scheme. In terms of line planning cost, the optimization scheme is markedly better than scheme 1 and scheme 2, and marginally better than scheme 3. In terms of the comprehensive stability margin, the optimized scheme is significantly better than the other 3 schemes.

Comparing the four schemes, the line impedance planning model based on the comprehensive stability margin of the power system is in a partial system scenario of a power grid. The optimized solution obtained by the solution achieves the best stable operating state of the system under the planning conditions and achieves good economy and scalability. Therefore, if in the planning and construction stage of the power grid, reasonable planning of line impedance is carried out according to the strategy proposed in this article. According to the line impedance value obtained by the optimized planning, the power grid is planned and constructed, which can effectively reduce the risk of transient instability and short-circuit current exceeding the standard. This scheme should be considered for future planning of real power grids in the future.

V. CONCLUSION

Transient instability and excessive short-circuit current are important factors that threaten the safe and stable operation of power grids. During power-grid planning, line impedance can effectively improve the system stability margin of a power grid. This article defines the transient stability margin and the short-circuit current margin, and relates these characteristics to establish an optimization model of the comprehensive stability margin. The external point penalty function method is used to determine the optimal planning impedance of the system, and the optimal comprehensive stability margin of the system is obtained, thereby improving the safety and stability margin of the system. The effectiveness of the proposed strategy is verified by an example of IEEE 10-generator 39-bus system and China's real power grid. The following conclusions can be drawn from the results of this study:

(1) The line impedance optimization planning method based on the comprehensive stability margin proposed in this paper can consider system transient instability and short-circuit current, exceeding the standard of other methods. This method yields superior performance to other control strategies that only solve transient instability or short-circuit current. Effective and unified coordination capabilities ensure the overall optimal and stable operation of the power grid.

(2) Line-impedance planning from the perspective of power-grid planning is achieved. While ensuring the stability of the system, this method has good economy and extensibility.

(3) While planning a future power grid, the strategy proposed in this article is applied to plan line impedance and current limiting measures. The proposed method can ensure the safety and reliability of the power grid and also provides a comprehensive stability margin, which improves the long-term sustainable and reliable development of the power grid. This study thus provides a reliable theoretical basis and solutions to avoid transient instability in a power grid and excessive short-circuit current during the planning of a power grid in the future.

Additionally, with the transformation of the world's energy structure, power grids are transforming into a new generation of systems that have a high proportion of new energy and power electronic equipment. This article is based on the electromechanical transient process, and we plan to research adding electromagnetic transient equations into the optimization model to avoid system instabilities caused by many electronic devices connected to the system during grid planning during operation. We thus seek a planning method that is more adaptable to electronics and that achieves better economic efficiency.

REFERENCES

[1] X. Shijie, "Consideration of technology for constructing Chinese smart grid," *Autom. Electr. Power Syst.*, vol. 33, no. 9, pp. 1–4, 2009.
[2] C. Xin, Y. Yan, X. Wei, J. Chu, H. Weijie, and L. Zuohong, "Evaluation index system of multi-infeed DC power grid planning schemes," *Guangdong Electr. Power*, vol. 31, no. 10, pp. 117–126, 2018.
[3] G. Shuai, R. Hongbo, and W. Qiong, "A review of planning, design and evaluation of regional integrated energy systems," *Shanghai Energy Conservation*, vol. 364, no. 4, pp. 245–250, 2019.
[4] Y. Li, B. Feng, G. Li, J. Qi, D. Zhao, and Y. Mu, "Optimal distributed generation planning in active distribution networks considering integration of energy storage," *Appl. Energy*, vol. 210, pp. 1073–1081, Jan. 2018.
[5] S. Teimourzadeh and F. Aminifar, "MILP formulation for transmission expansion planning with short-circuit level constraints," *IEEE Trans. Power Syst.*, vol. 31, no. 4, pp. 3109–3118, Jul. 2016.
[6] C. Lili, H. Minxing, Z. Hong, G. Deqing, H. Yongning, and T. Bei, "An optimization strategy for limiting short circuit current," *Autom. Electr. Power Syst.*, vol. 33, no. 11, pp. 38–42, 2009.
[7] X. Xian, D. Tao, and W. Qiulan, "220kV power grid district-dividing optimization for limiting fault current," *Autom. Electr. Power Syst.*, vol. 33, no. 22, pp. 98–101, 2009.
[8] B. Song and J. Gu, "A Bi-level expansion planning model of transmission systems considering short-circuit current constraints," *Trans. China Electrotech. Soc.*, vol. 31, no. 7, pp. 92–101, 2016.
[9] M. Pavella, D. Ernst, and D. Ruiz-Vega, *Transient Stability of Power Systems : A Unified Approach to Assessment and Control*. New York, NY, USA: Springer, 2000.
[10] P. N. Vovos, G. P. Harrison, A. R. Wallace, and J. W. Bialek, "Optimal power flow as a tool for fault level-constrained network capacity analysis," *IEEE Trans. Power Syst.*, vol. 20, no. 2, pp. 734–741, May 2005.
[11] M. Dengkai, W. Tong, X. Yuwei, and D. Wenjuan, "Elastic net based online assessment of power system transient stability margin," *Power Syst. Technol.*, vol. 44, no. 1, pp. 19–26, 2020.
[12] Y. Dequan, J. Hongjie, and Z. Shuai, "Power system transient stability assessment and stability margin prediction basedon compound neural network," *Autom. Electr. Power Syst.*, vol. 37, no. 20, pp. 41–46, 2013.
[13] Y. Li and Z. Yang, "Application of EOS-ELM with binary jaya-based feature selection to real-time transient stability assessment using PMU data," *IEEE Access*, vol. 5, pp. 23092–23101, 2017.
[14] X. Zhang, Z. Zhu, Y. Fu, and W. Shen, "Multi-objective virtual inertia control of renewable power generator for transient stability improvement in interconnected power system," *Int. J. Electr. Power Energy Syst.*, vol. 117, May 2020, Art. no. 105641.
[15] Y. Xueyan, Y. Jiongcheng, L. Yutian, and Q. Chenguang, "Deep learning based transient stability assessment and severity grading," *Electr. Power Autom. Equip.*, vol. 38, no. 05, pp. 64–69, 2018.
[16] J. Lv, M. Pawlak, and U. D. Annakkage, "Prediction of the transient stability boundary using the lasso," *IEEE Trans. Power Syst.*, vol. 28, no. 1, pp. 281–288, Feb. 2013.
[17] T. Han, Y. Chen, J. Ma, Y. Zhao, and Y.-Y. Chi, "Surrogate modeling-based multi-objective dynamic VAR planning considering short-term voltage stability and transient stability," *IEEE Trans. Power Syst.*, vol. 33, no. 1, pp. 622–633, Jan. 2018.
[18] T. Han, Y. Chen, and J. Ma, "Multi-objective robust dynamic VAR planning in power transmission girds for improving short-term voltage stability under uncertainties," *IET Gener., Transmiss. Distrib.*, vol. 12, no. 8, pp. 1929–1940, Apr. 2018.
[19] Y. Xu, R. Zhang, J. Zhao, Z. Y. Dong, D. Wang, H. Yang, and K. P. Wong, "Assessing short-term voltage stability of electric power systems by a hierarchical intelligent system," *IEEE Trans. Neural Netw. Learn. Syst.*, vol. 27, no. 8, pp. 1686–1696, Aug. 2016.
[20] M. Peker, A. S. Kocaman, and B. Y. Kara, "Benefits of transmission switching and energy storage in power systems with high renewable energy penetration," *Appl. Energy*, vol. 228, pp. 1182–1197, Oct. 2018.
[21] O. Ziaee and F. Choobineh, "Optimal location-allocation of TCSCs and transmission switch placement under high penetration of wind power," *IEEE Trans. Power Syst.*, vol. 32, no. 4, pp. 3006–3014, Jul. 2017.
[22] Y. Zheng, J. Zhao, Y. Song, F. Luo, K. Meng, J. Qiu, and D. J. Hill, "Optimal operation of battery energy storage system considering distribution system uncertainty," *IEEE Trans. Sustain. Energy*, vol. 9, no. 3, pp. 1051–1060, Jul. 2018.
[23] F. Qiu and J. Wang, "Chance-constrained transmission switching with guaranteed wind power utilization," *IEEE Trans. Power Syst.*, vol. 30, no. 3, pp. 1270–1278, May 2015.
[24] W. Xiaoming, D. Liu, J. Wu, Y. Huang, and L. Yun, "Energy function-based power system transient stability analysis," *Power Syst. Technol.*, vol. 35, no. 8, pp. 114–118, 2011.
[25] Y. Liu, "Analysis and quantification of transient stability of power system with wind farm based on heuristic energy function," M.S. thesis, School Automat. Eng., Univ. Electron. Sci. Technol. China, Chengdu, China, 2020.
[26] H. Wentao, D. Changhong, W. Zhiqiang, S. Zhengyu, and W. Yixuan, "A real-time strategy for under frequency pump shedding of pumped power storage station based on external point function method," *Proc. CSEE*, vol. 33, no. 16, pp. 104–111, Jun. 2013.
[27] Y. Lin, R. Xue, and Z. Chengjie, "Research on optimization of distribution network voltage fluctuation based on penalty function method," *Internet Things Technol.*, vol. 9, no. 5, pp. 96–98, 2019.

DAHU LI received the Ph.D. degree in power systems and automation from the Huazhong University of Science and Technology, Wuhan, China, in 2006.

He is currently working with State Grid Hubei Electric Power Company Ltd., China, where he obtained professor-level Senior Engineer. His main research directions include power system security and stability analysis, new energy and the energy Internet planning, and design and scheduling. He has been awarded professional leading talents, and engineering technical experts of State Grid Hubei Electric Power Company Ltd. He won one second prize of China's National Science and Technology Progress Award, five provincial and ministerial science and technology progress awards, and compiled one group standard of China Electrical Engineering Association.

SHUAI YANG was born in Chongqing, China, in 1995. He received the B.S. degree in electrical engineering and automation from Chongqing Three Gorges University, Chongqing, China, in 2018. He is currently pursuing the M.S. degree in electrical engineering with the Hubei University of Technology, Wuhan, China.

His main research interests include integrated energy systems, and power system operation and control.

WENTAO HUANG was born in Wuhan, Hubei, China, in 1984. He received the B.S. and M.S. degrees in electrical engineering and the Ph.D. degree in power systems and automation from Wuhan University, in 2007 and 2013, respectively. Since 2013, he has been working with State Grid Hubei Electric Power Company, engaged in the analysis and calculation of the operation mode of the power grid. He has won several second prize of scientific and technological progress of State Grid Hubei Electric Power Company.

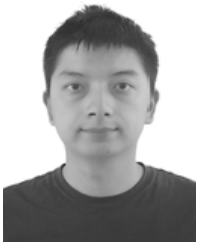

JUN HE (Member, IEEE) received the B.S. degree in energy and power engineering and a minor in computer science and technology from the Huazhong University of Science and Technology, Wuhan, China, in 2007, and the Ph.D. degree in power systems and automation from Wuhan University, in 2014. He has worked with State Grid Hubei Electric Power Company Ltd., where he obtained a senior engineer position. His main research directions include power system security and stability analysis, new energy and the energy Internet planning, and design and scheduling. He has won power grid regulation and control work advanced individuals of the State Grid Corporation of China Hubei Company, in 2016. He has participated in the preparation of the ITU Standard Microgrid Planning and Design Guidelines. He has won the second prize of scientific and technological progress of the Hubei provincial government.

ZHIJUN YUAN was born in Chongqing, China, in 1997. He received the B.S. degree in electrical engineering and automation from Chongqing Three Gorges University, Chongqing, China, in 2019. He is currently pursuing the M.S. degree in electrical engineering with the Hubei University of Technology, Wuhan, China.

His main research interests include integrated energy systems, and power system operation and control.

JINMAN YU was born in Chongqing, Chongqing, China, in 1996. She received the B.S. degree in electrical engineering and automation from Chongqing Three Gorges University, Chongqing, China, in 2019. She is currently pursuing the M.S. degree in electrical engineering with the Hubei University of Technology, Wuhan, China.

Her main research interests include power system frequency emergency control, and power system operation and control.